Theses   Electronic Theses and Dissertations

4-2017

Unwrapping MRI Phase by Using Multi-Echo Technique

Shamma Ali Rashed Ali Al Hassani

Follow this and additional works at: https://scholarworks.uaeu.ac.ae/all_theses

Part of the Physics Commons

UAEU

جامعة الإمارات العربية المتحدة
United Arab Emirates University

United Arab Emirates University

College of Science

Department of Physics

UNWRAPPING MRI PHASE BY USING MULTI-ECHO TECHNIQUE

Shamma Ali Rashed Ali Al Hassani

This thesis is submitted in partial fulfilment of the requirements for the degree of Master of Science in Physics

Under the Supervision of Professor Bashar Issa

April 2017

Declaration of Original Work

I, Shamma Ali Rashed Ali Al Hassani, the undersigned, a graduate student at the United Arab Emirates University (UAEU), and the author of this thesis entitled *"Unwrapping MRI Phase by Using Multi-Echo Technique"*, hereby, solemnly declare that this thesis is my own original research work that has been done and prepared by me under the supervision of Professor Bashar Issa, in the College of Science at UAEU. This work has not previously been presented or published, or formed the basis for the award of any academic degree, diploma or a similar title at this or any other university. Any materials borrowed from other sources (whether published or unpublished) and relied upon or included in my thesis have been properly cited and acknowledged in accordance with appropriate academic conventions. I further declare that there is no potential conflict of interest with respect to the research, data collection, authorship, presentation and/or publication of this thesis.

Student's Signature: _____   Date: __22 May 2017__

Approval of the Master Thesis

This Master Thesis is approved by the following Examining Committee Members:

1) Advisor (Committee Chair): Professor Bashar Issa

   Title: Professor

   Department of Physics

   College of Science
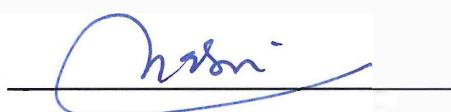
   Signature _____ Date 27/4/2017

2) Member: Professor Salah Nasri

   Title: Professor

   Department of Physics

   College of Science

   Signature _____ Date 27/4/2017

4) Member (External Examiner): Dr Usman Tariq

   Title: Assistant Professor

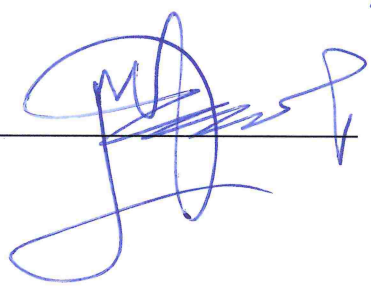   Department of Electrical Engineering

   Institution: American university of Sharjah, Sharjah, UAE
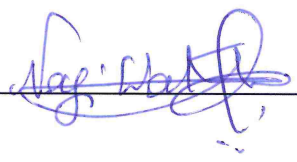
   Signature _____ Date 27/04/17

This Master Thesis is accepted by:

Dean of the College of Science: Professor Ahmad Murad

Signature _____ Date _22/5/ 2017_

Dean of the College of Graduate Studies: Professor Nagi T. Wakim

Signature _____ Date _23/5/ 2017_

Copy _8_ of _8_

Abstract

Phase unwrapping is a classic signal processing problem and an unavoidable procedure that can be faced with in a variety of applications which are interested in the phase, such as synthetic aperture radar (SAR), field mapping in magnetic resonance imaging (MRI), wavefront distortion measurement of adaptive optics, interferometry, and surface shape measurement. Although phase unwrapping is one of the most challenging tasks in signal processing because of the presence of residues, noise in the data, discontinuities or other phase particularities, there are many successful phase unwrapping techniques and algorithms that have been developed in the last decades. In this thesis, we present a modified algorithm based on the Andris's method which is dependent on the difference in two echo times (TE). The proposed algorithm is confirmed by using simulated phase MR data which are highly distorted by large magnetic field inhomogeneity (ΔB) or long echo time (TE). The approach is evaluated by comparison to other unwrapping algorithms and results show that the proposed algorithm has better accuracy.

Keywords: Phase unwrapping, inhomogeneity, echo time, MRI.

Title and Abstract (in Arabic)

إزالة الالتباس والتكرار الزاوي في التصوير بالرنين المغناطيسي باستخدام تقنية متعددة الصدى

الملخص

إن إزالة الإلتباس و التكرار الزاوي (Phase Unwrapping) هي مشكلة كلاسيكية في معالجة الإشارات وإجراء لا مفر منه قد تواجهه في مجموعة متنوعة من التطبيقات التي لديها اهتمام في الطور phase، مثل الرادار ذي الفتحة الاصطناعية (SAR)، ورسم الخرائط المجالية في التصوير بالرنين المغناطيسي (MRI)، وقياس واجهة الموجة التشويه البصريات التكيفية، التداخل، وقياس شكل السطح. على الرغم من أن إزالة الإلتباس و التكرار الزاوي (Phase Unwrapping) هي واحدة من أصعب المهام في معالجة الإشارات بسبب وجود بقايا والضوضاء في البيانات، انقطاعات أو غيرها من خصائص الطور (phase) وهناك العديد من التقنيات و العمليات الناجحة لإزالة الإلتباس و التكرار الزاوي (Phase Unwrapping) التي تم تطويرها في آخر عقود. في هذه الرسالة نقدم طريقة معدلة على أساس طريقة Andris التي تعتمد عل الفرق في أوقات الصدى ((echo time (TE). وتم التأكد من فعالية الطريقة المقترحة باستخدام محاكاة لبيانات MR التي يتم تشويهها بشكل كبير من قبل:عدم التجانس الكبير (ΔB) أو وقت الصدى (TE) الطويل. وتمت مقارنتها بعدة أساليب أخرى تبين أن الطريقة المقترحة لها دقة أفضل.

مفاهيم البحث الرئيسية: إزالة الإلتباس و التكرار الزاوي (Phase Unwrapping)، أوقات الصدى (echo (times (TE)، المجال المغناطيسي الغير متجانس، التصوير بالرنين المغناطيسي.

Acknowledgements

This project would not have been possible without the support of many people. I would like to thank my committee for their guidance, support, and assistance throughout my preparation of this thesis, especially my advisor Professor Bashar Issa, who introduced me to the exciting field of Magnetic Resonance Imaging (MRI) and whose endless ideas and encouragement led to this.

I would like to thank the chair and all members of the Department of science at the United Arab Emirates University for assisting me all over my studies and research.

Special thanks go to my parents, brothers, sisters, and colleagues who helped me along the way.

Dedication

To my beloved parents, family, and friends

Table of Contents

List of Tables

List of Figures

List of Abbreviations

CPULSI	Calibrated Phase Unwrapping based on Least-Squares and Iterations
TE	Echo Time
ΔTE	Echo time differences
GRE	Gradient-echo
γ	Gyromagnetic ratio
ΔB	Magnetic field inhomogeneity
MRI	Magnetic Resonance Imaging
MSE	Mean Squared Error
MPULSI	Modified Phase Unwrapping based on Least Squares and Iterations
NMR	Nuclear Magnetic Resonance
$\emptyset_{err}$	Phase error
ρ	Proton density
SAR	Synthetic Aperture Radar
$\Delta\varphi$	The resulting unwrapped phase
UMPIRE	Unwrapping Multi-echo Phase Images with iRregular Echo spacing

Chapter 1: Introduction

1.1 Overview

The spatial frequency transform is one of the most significant and widely applied tools for image representation and analysis. It can be represented in terms of magnitude and phase. The magnitude and the phase of a signal are important quantities, but usually the phase has been ignored in favor of magnitude as is widely used in medical imaging. In some cases, the important features of a signal are conserved only if the phase is preserved. In addition, phase contains more information related to signal structure than magnitude does, especially in the case of images. The highly impregnable to noise and contrast distortions of the phase is a feature required in image processing. The significance of phase information on images has inspired its application for different tasks such as image segmentation, edges detection, etc. There are many image processing applications in interferometry, medical, military, and industrial areas that depend on the extracted phase signal from their input image, for example: synthetic aperture radar (SAR), field mapping in magnetic resonance imaging (MRI), wavefront distortion measurement of adaptive optics, interferometry, and surface shape measurement [1-2].

1.2 The Phase Unwrapping Problem

Many applications that are interested in the phase signal use modern algorithms to extract it. However the phase suffers from 2π jumps due to the numerical operations based on the arctangent function, which produces a wrapped output problem. The ideal phase should be continuous and increasing or decreasing relatively slowly, but if there is a wrapping problem there will be a 2π discontinuity

of the extracted phase. This "wrapping" problem means that the measured phase signal can only be within 2π range which is called the wrapped phase, while the original (undetected) phase signal can take any value [3-4].
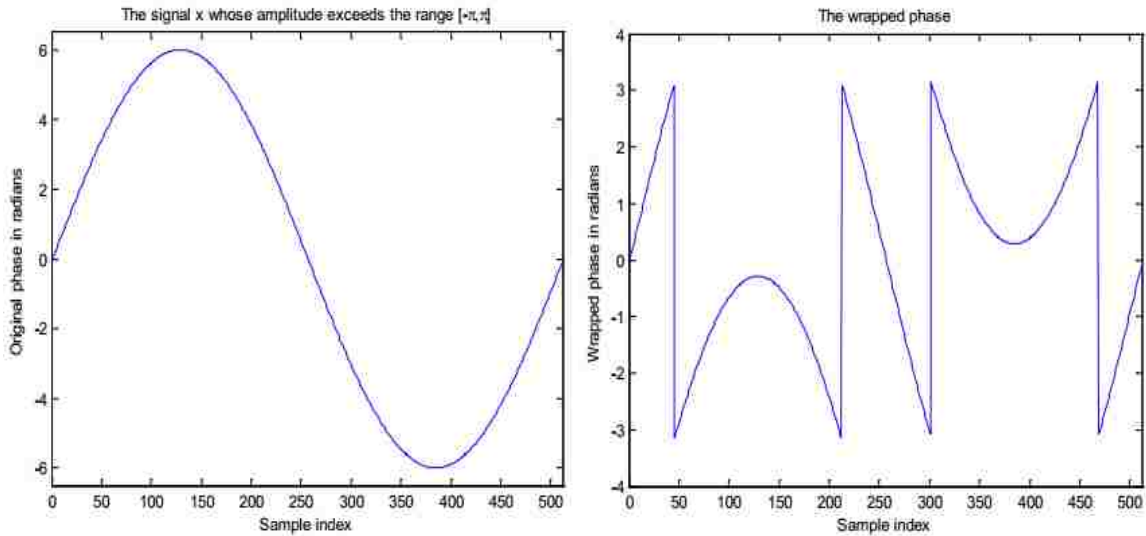
There are thousands of individual phase wraps in each image. A phase wrap can be either 'fake phase wrap' or a 'genuine phase wrap' that has been produced by the presence of noise and sometimes by the phase extraction algorithm itself. As Figure 1(b) shows the phase wraps that in the phase signal must be removed and return the phase signal to a continuous form as Figure 1(a) and hence make the phase usable in any processing. This process is called the phase unwrapping [3].

The unwrapped phase at the grid point (i,j) of a phase map is defined as

$$\varphi_{ij} = \emptyset_{ij} + 2\pi k_{ij} \qquad -\pi < \emptyset_{ij} \leq \pi \qquad (1)$$

where $\emptyset_{ij}$ is the wrapped phase and k_{ij} is an integer [2].

The failure or success of the unwrapping procedure can have a great effect on the performance of systems interested in the phase extraction process. Although the phase unwrapping is not a new topic, it is a difficult task for many reasons. First,

distinguishing between genuine and fake phase wraps is so difficult and this adds complication to the phase unwrapping. Another important reason, the phase unwrapping is accumulative and the image is processed consecutively pixel-by-pixel. If there is a genuine phase wrap between two pixels, or a fake phase wrap in the phase map, an error will occur in unwrapping both pixels and it will reproduce through the rest of the image. Even if all the wraps in the image have been unwrapped successfully except one, it is possible that the image could be totally unusable. The phase unwrapping process has very strict requirements on the algorithms that are designed to accomplish this task because of this accumulative property. In fact, phase unwrapping is believed to be one of the most difficult problems of both mathematics and engineering. Since 1990s, a huge amount of effort has been devoted by different researchers who have applied numerous algorithms, with very wide range of mathematical and engineering theory, as solutions to the phase unwrapping problem. Number theory, graph theory, network flow algorithms, the Fourier transform, and statistical approaches are examples of theoretical principles that have been used in signal and image processing algorithms [2, 5].

1.3 The Phase Unwrapping Algorithms

In the last decade, many journal papers have been published suggesting solutions to the phase unwrapping problem. Many phase unwrapping approaches were developed and show the best performance in the presence of noise among them, minimum L^p-norm (L^0), Flynn's minimum discontinuity, and quality-guided algorithm. In addition, spatial filtering can be used to reduce and clean the wrapped phase map in the presence of high noise before the unwrapping process but filtering

algorithms may get rid of some useful information. This section provides an outline of the algorithmic details of different methods and a short discussion [5].

1.3.1 UMPIRE

A group of scientists in the Medical University of Vienna in Austria developed a method of unwrapping phase images that works in the presence of several wraps between echoes, and generate unwrapped phase images of multi-echo scan. Unwrapping Multi-echo Phase Images with iRregular Echo spacings (UMPIRE) is a fast, conceptually simple, and reliable method to generate wrap-free phase images. It requires a multi gradient echo of three unequally spaced echoes such that the evaluated phase in that time within the range $-\pi$ to $+\pi$ in all voxels of interest. Under this condition, no wraps occur the phase image in the two inter-echo periods which is used as a basis of knowledge of the ideal range of ΔB values. The estimated ΔB can be used to differentiate and remove wraps in phase images [6].

1.3.2 MPULSI or CPULSI

MPULSI (Modified Phase Unwrapping based on Least Squares and Iterations) or CPULSI (Calibrated Phase Unwrapping based on Least-Squares and Iterations) are algorithms based on least-squares, iteration and phase calibration. In the presence of high noise, it is difficult to remove generated error by filtering, so the calibration approach is required. The least-squares methods reach the unwrapped phase that minimizes the differences between the discrete derivatives of the wrapped phase and those of the unwrapped solution. The phase error $\Delta\Psi_{ij,k}$ defined as

$$\Delta\Psi_{ij,k} = \varphi_{ij,k} \ - \ \emptyset_{ij,k} \qquad\qquad (2)$$

where $\varphi_{ij,k}$ is the least-squares unwrapped phase, $\emptyset_{ij,k}$ is the calibrated unwrapped phase at the grid point (i,j) of a phase map and k is the iteration number. If the calibrated unwrapped phase is continuous, it will be the true phase. On the other hand, if both the least-squares and the calibrated unwrapped phase have the same wrap counts, the phase error ($\Delta\Psi_{ij,k}$) will be within the range $[-\pi, +\pi]$ or wrapped into $[-\pi, +\pi]$. Therefore if the phase error is wrapped, the calibrated unwrapped phase will also be discontinuous and not equal to the true phase. Using the least-squares algorithm to unwrap the phase error added to the previous least squares unwrapped phase to have unwrapped results closer to the true phase. Therefore, the iteration process requires to continue until the unwrapped phase being the closest to the true phase [4-5].

1.3.3 Phase Unwrapping Method Based on Network Programming

The derivatives of the unwrapped phase are evaluated with an error, an integer multiple of 2π, see page 2 equation (1). A new phase unwrapping method based on network programming depends on this fact such that the phase unwrapping is formulated as a global minimization problem with integer variables. Minimizing the weighted deviation between the evaluated and the unknown discrete derivatives of the unwrapped phase, but the two functions must differ by integer multiples of 2π. With this condition, it should prevent the diffusion of errors and identify the resultant unwrapped phase to the original phase. The unwrapped phase results of this method are less sensitive to small changes of the weighting mask used [7].

In this thesis, we present a modified algorithm based on the Andris method which is dependent on the difference in two echo times (TE). The proposed algorithm is confirmed by using simulated phase MR data which are highly distorted

by large magnetic field inhomogeneity (ΔB) or long echo time (TE). The approach is evaluated by comparison to other unwrapping algorithms and results show that the proposed algorithm has better accuracy. This thesis is organized as follows: in Chapter 2, we describe the theoretical basics for the modified phase unwrapping algorithm; Chapter 3 shows and discusses the results of simulation of the corrupted phase with large magnetic field inhomogeneity (ΔB) or long echo time (TE). Also, there is a discussion on the evaluation of the proposed approach with comparison with other established unwrapping algorithms given in Chapter 4. Conclusions to the study are shown in Chapter 5.

Chapter 2: Methods

2.1 The Phase

After MR measurement, an element of the data matrix describing the signal can be given by

$$I = k \rho \exp\big(i(-\gamma \, \Delta B \, TE + \emptyset_{err})\big) \tag{3}$$

where k is related to electronic gain, and will be assumed unity from now on, ρ is proton density, γ is the gyromagnetic ratio, ΔB is the inhomogeneity of the static magnetic field within a voxel, TE is the echo time, and $\emptyset_{err}$ is the phase error, which appears because of gradients (*y*- and *x*- gradients) or RF sources. The phase can be calculated as an argument of the complex data

$$\emptyset = \arg(I) = -\gamma \, \Delta B \, TE + \emptyset_{err} \tag{4}$$

$\emptyset_{err}$ is usually small compared to the first term in the RHS in a well-tuned MRI scanner. The exponential function of an imaginary variable is periodic, i.e.

$$-\pi \leq -\gamma \, \Delta B \, TE + \emptyset_{err} \leq \pi \tag{5}$$

The phase depends on the inhomogeneity ΔB and echo time TE. If ΔB is large or TE is long, the periodicity distorts the result and phase wrapping appears in the phase angle. That is even when the true phase has a value greater than π, the detected phase value after calculating the arctangent will only be within $|\pi|$. Furthermore, as ΔB and TE become larger and larger the severity of the phase wrapping becomes stronger. While some phase unwrapping techniques will work with moderate phase wrapping, they will fail when the wrapping becomes severe.

This makes it necessary to improve existing techniques and design new more efficient ones. As mentioned previously in the introduction, the presence of the phase wrapping problem makes the phase discontinuous and unusable. Therefore, phase unwrapping is a necessary process [8].

As it is known, the inhomogeneity ΔB is uncontrollable because it is proportional to the susceptibility χ of the tissues. Therefore, we can reduce the distortion of the phase by shortening the echo time (TE) although this is dependent on the MRI sequence and the objective of the scan. For example, the echo time (TE) has to be large in functional MRI where image T_2-weighting is required. It should be noted, the phase error ($\emptyset_{err}$) may distort the results also.

2.2 The Andris Method

In Andris method, the wrapping can be removed by shortening the effective echo time. The MR signal from the gradient-echo (GRE) sequence is acquired twice, with different echo times TE_1 and TE_2 with as small difference between them as possible. This difference will obviously depend on the machine both hardware and software. After the Fourier transform, the following values of data are obtained

$$I_1 = \rho \exp(i(-\gamma \, \Delta B \, TE_1 + \emptyset_{err1})) = I_{1re} + iI_{1im} \qquad (6)$$

$$I_2 = \rho \exp\big(i(-\gamma \, \Delta B \, TE_2 + \emptyset_{err2})\big) = I_{2re} + iI_{2im} \qquad (7)$$

where we choose ΔB as a linear function of x and y variables

$$\Delta B = \Delta B_o \big(2 \, \text{peaks(N)}\big)(0.1 \, x + 0.01 \, y) \qquad (8)$$

where the "peaks" is a MATLAB function used to generate the continuous phase image. The ratio of both values is calculated as

$$\frac{I_1}{I_2} = \rho \exp\left(i\,\gamma\,\Delta B(TE_2 - TE_1) + \emptyset_{err\_res}\right) \tag{9}$$

$$= \frac{I_{1re} \cdot I_{2re} + I_{1im} \cdot I_{2im}}{I_{2re}^2 + I_{2im}^2} + i\,\frac{I_{1im} \cdot I_{2re} - I_{1re} \cdot I_{2im}}{I_{2re}^2 + I_{2im}^2} \tag{10}$$

Or its complex conjugate

$$\frac{I_2}{I_1} = \rho \exp\left(i\,\gamma\,\Delta B(TE_1 - TE_2) - \emptyset_{err\_res}\right) \tag{11}$$

$$= \frac{I_{1re} \cdot I_{2re} + I_{1im} \cdot I_{2im}}{I_{1re}^2 + I_{1im}^2} + i\,\frac{I_{1re} \cdot I_{2im} - I_{1im} \cdot I_{2re}}{I_{1re}^2 + I_{1im}^2} \tag{12}$$

where $\emptyset_{err\_res} = \emptyset_{err1} - \emptyset_{err2}$. We will assume that $\emptyset_{err1} = \emptyset_{err2}$ and $|\emptyset_{err\_res}| \cong$ 0 in further calculations. In a later section we will investigate the effect of $\emptyset_{err}$ where it is caused by a linear gradient in x-direction. The phase of the ratio can be calculated as an argument of the complex data

$$\arg\left(\frac{I_1}{I_2}\right) \quad or \quad \arg\left(\frac{I_2}{I_1}\right) \tag{13}$$

The range of values satisfies the following condition:

$$-\pi \le \arg\left(\frac{I_1}{I_2}\right) \le \pi$$

$$or \quad -\pi \le \arg\left(\frac{I_2}{I_1}\right) \le \pi \tag{14}$$

if and only if, the difference in the echo times ($\Delta TE_{12} = |TE_2 - TE_1|$) is sufficiently short. The difference in the echo times (ΔTE_{12}) is called the effective echo time between TE_1 and TE_2. The resulting unwrapped phase ($\Delta\varphi$) per ΔTE_{12}, is given by

$$\Delta\varphi = \tan^{-1}\left(\frac{I_{2re}I_{1im} - I_{1re}I_{2im}}{I_{1re}I_{2re} + I_{1im}I_{2im}}\right) \tag{15}$$

The phase wrapping is removed similarly to sequences using echo time shortening because the effective TE is short due to division ($\Delta TE_{12} \ll TE_1, TE_2$). The phase of the MR data corresponding to a voxel from the first and second measurements are given by

$$\varphi_1 = \Delta\varphi \times \left(\frac{TE_1}{\Delta TE_{12}}\right) \tag{16}$$

$$\varphi_2 = \Delta\varphi \times \left(\frac{TE_2}{\Delta TE_{12}}\right) \tag{17}$$

where φ_1 and φ_2 are the unwrapped phase of signals 1 and 2, respectively [9].

2.2.1 The Effect of Random Noise

As explained previously in the introduction, the presence of noise in the signal can worsen the phase unwrapping process. This is so because a single error in determining only one phase wrap may affect the whole signal due to propagation of errors. The effect of random (white) noise on the effectiveness of unwrapping will be investigated. The white noise (Noise) was added into the whole image

$$I_1 = \rho \exp(i(-\gamma \, \Delta B \, TE_1 + \emptyset_{err1})) + \text{Noise} \tag{18}$$

$$I_2 = \rho \exp(i(-\gamma \, \Delta B \, TE_2 + \emptyset_{err2})) + \text{Noise} \tag{19}$$

The mean squared error (MSE) was calculated to study the effect of adding the noise on the phase unwrapping process

$$MSE = \frac{\sum_i^N (\text{diff})^2}{N} \tag{20}$$

where diff is the difference between the correct phase, if available, and the unwrapped phase using the Andris' method and N is the number of samples. The

MSE of each signal is

$$MSE1 = \frac{\sum_i^N(-\gamma\,\Delta B\,TE_1 - \varphi_1)^2}{N} \qquad (21)$$

$$MSE2 = \frac{\sum_i^N(-\gamma\,\Delta B\,TE_2 - \varphi_2)^2}{N} \qquad (22)$$

where $-\gamma\,\Delta B\,TE_1$ and $-\gamma\,\Delta B\,TE_2$ are the correct phase, if available, and φ_1 and φ_2 are the unwrapped phase of signals 1 and 2, respectively.

The Andris method using two different TE values works with certain range of parameters until it fails due to large wraps when TEs are very long or the inhomogeneity ΔB is very large. Then, the resultant phase of Andris' method will still have wraps. So we modified the Andris method to unwrap the remaining phase that appears due to large ΔB and long TEs.

2.3 The Modified Andris Method

In the modified Andris method, instead of using the difference between two echo times we use the differences between three echo times to eliminate the wrapping when we have large inhomogeneity ΔB or long TE and the original Andris method does not work.

After simulating three signals with different echo times ($TE_1, TE_2,$ and TE_3), the Andris method was applied twice, first between signals 1 and 2 and secondly between signals 2 and 3. Then, applying Andris method third time to the resulting differences. We then calculate the unwrapped phase ($\Delta\varphi$).

The three simulated signals

$$I_1 = k \, \rho \, \exp(i(-\gamma \, \Delta B \, TE_1 + \emptyset_{err1})) + Noise = I_{1re} + iI_{1im} \qquad (23)$$

$$I_2 = k \, \rho \, \exp\big(i(-\gamma \, \Delta B \, TE_2 + \emptyset_{err2})\big) + Noise = I_{2re} + iI_{2im} \qquad (24)$$

$$I_3 = k \, \rho \, \exp\big(i(-\gamma \, \Delta B \, TE_3 + \emptyset_{err3})\big) + Noise = I_{3re} + iI_{3im} \qquad (25)$$

The ratio of signals 1 and 2 is calculated as

$$\frac{I_1}{I_2} = \rho \, \exp\big(i \, \gamma \, \Delta B (TE_2 - TE_1) + \emptyset_{err\_res}\big) \qquad (26)$$

$$= \frac{I_{1re} \cdot I_{2re} + I_{1im} \cdot I_{2im}}{I_{2re}{}^2 + I_{2im}{}^2} + i \, \frac{I_{1im} \cdot I_{2re} - I_{1re} \cdot I_{2im}}{I_{2re}{}^2 + I_{2im}{}^2} \qquad (27)$$

and the ratio of signals 2 and 3

$$\frac{I_2}{I_3} = \rho \, \exp\big(i \, \gamma \, \Delta B (TE_3 - TE_2) + \emptyset_{err\_res}\big) \qquad (28)$$

$$= \frac{I_{2re} \cdot I_{3re} + I_{2im} \cdot I_{3im}}{I_{3re}{}^2 + I_{3im}{}^2} + i \, \frac{I_{2im} \cdot I_{3re} - I_{2re} \cdot I_{3im}}{I_{3re}{}^2 + I_{3im}{}^2} \qquad (29)$$

Then the ratio of the resulting differences eq. (26) and (28)

$$\frac{I_{12}}{I_{23}} = \rho \, \exp\big(i \, \gamma \, \Delta B (-TE_1 + 2 \, TE_2 - TE_3) + \emptyset_{err\_res}\big) \quad (30)$$

$$= \frac{I_{12re} \cdot I_{23re} + I_{12im} \cdot I_{23im}}{I_{23re}{}^2 + I_{23im}{}^2}$$

$$+ i \, \frac{I_{12im} \cdot I_{23re} - I_{12re} \cdot I_{23im}}{I_{23re}{}^2 + I_{23im}{}^2} \qquad (31)$$

where $I_{12} = \frac{I_1}{I_2}$ and $I_{23} = \frac{I_2}{I_3}$. We will assume that $\emptyset_{err1} = \emptyset_{err2} = \emptyset_{err3}$ and $\left| \emptyset_{err\_res} \right| \cong 0$ in further calculations. The resulting unwrapped phase $(\Delta\varphi)$, is given by

$$\Delta\varphi_{12} = \tan^{-1}\left(\frac{I_{2re}I_{1im} - I_{1re}I_{2im}}{I_{1re}I_{2re} + I_{1im}I_{2im}}\right) \tag{32}$$

$$\Delta\varphi_{23} = \tan^{-1}\left(\frac{I_{3re}I_{2im} - I_{2re}I_{3im}}{I_{2re}I_{3re} + I_{2im}I_{3im}}\right) \tag{33}$$

$$\Delta\varphi_{eff} = \tan^{-1}\left(\frac{I_{23re}I_{12im} - I_{12re}I_{23im}}{I_{12re}I_{23re} + I_{12im}I_{23im}}\right) \tag{34}$$

where $\Delta\varphi_{12}, \Delta\varphi_{23}$, and $\Delta\varphi_{eff}$ are the resulting unwrapped phase of ratio eq. (27, 29, and 31), respectively. The phase wrapping is removed because $\Delta TE_{12}, \Delta TE_{23}$, and ΔTE_{eff} are short.

$$\Delta TE_{12} = TE_2 - TE_1 \tag{35}$$

$$\Delta TE_{23} = TE_3 - TE_2 \tag{36}$$

$$\Delta TE_{eff} = \Delta TE_{12} - \Delta TE_{23} \tag{37}$$

The phase of the signals 1, 2, and 3 is given by

$$\varphi_1 = \Delta\varphi_{eff} \times \left(\frac{TE_1}{\Delta TE_{eff}}\right) \tag{38}$$

$$\varphi_2 = \Delta\varphi_{eff} \times \left(\frac{TE_2}{\Delta TE_{eff}}\right) \tag{39}$$

$$\varphi_3 = \Delta\varphi_{eff} \times \left(\frac{TE_{23}}{\Delta TE_{eff}}\right) \tag{40}$$

Copy of the MATLAB code is given in the appendix.

Chapter 3: Results

In order to evaluate the accuracy of the proposed unwrapping algorithm, a realistic numerical simulation was carried out. The aim of such simulation is to produce phase images with adequate probability to have wrapping problem by large inhomogeneity and long echo time. The performance of the Andris method has been tested using two simulated MR images in the absence of noise and phase error. The results are shown in Figures 2 and 3.
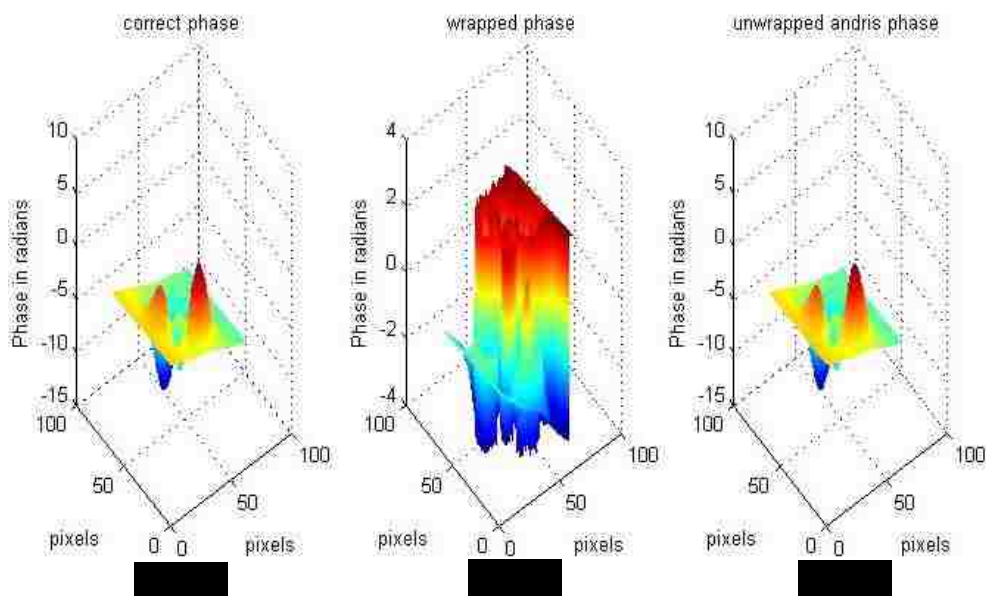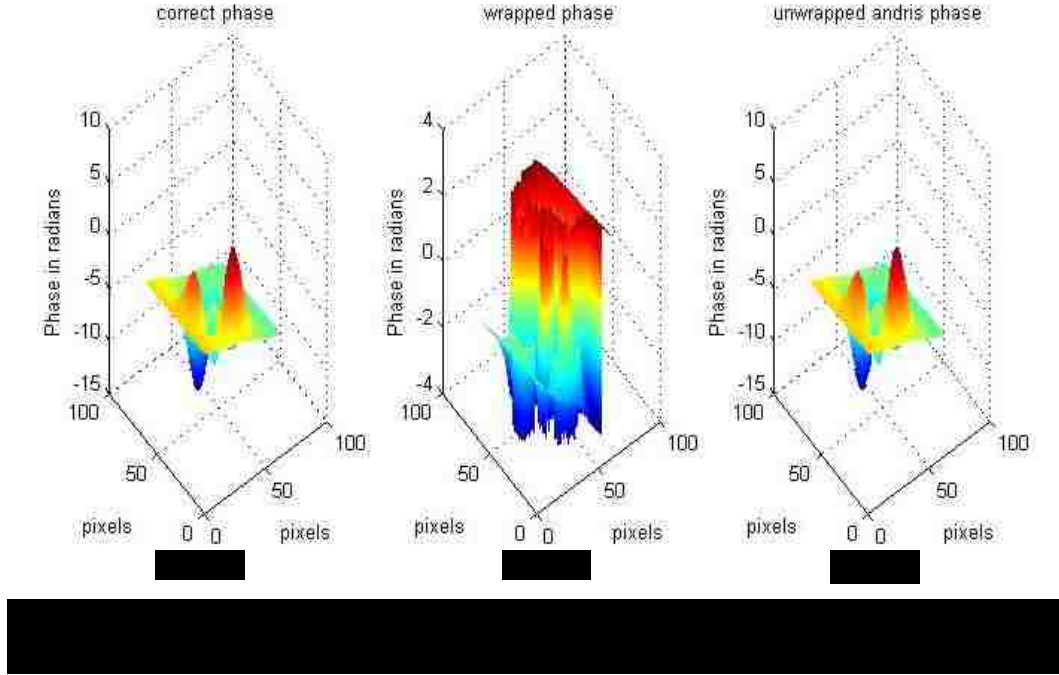
Figures 2(a) and 3(a) show the simulated correct phase of the images 1 and 2, respectively, at $TE_1 = 20$ ms, $\Delta B_0 = 10^{-7}$T and $\Delta TE_{12} = 2$ ms. Figures 2(b) and 3(b) represent the wrapped phase of the signal 1 and signal 2, respectively, prior to applying the Andris' method. Figures 2(c) and 3(c) are the unwrapped phase of the two signals 1 and 2, respectively, using the Andris method with no added noise or phase error.

It should be noted that the complex division between the phase of images 1 and 2, eq. (6) and (7) by using argument subtraction:

$$\arg(I_1) - \arg(I_2) = \rho \exp\big(i\,\gamma\,\Delta B(\Delta TE)\big) \qquad (41)$$

will not unwrap the images for all values of ΔTE; it works just for very very small ΔTE. The division using subtraction distorts the result, see Figure 4.
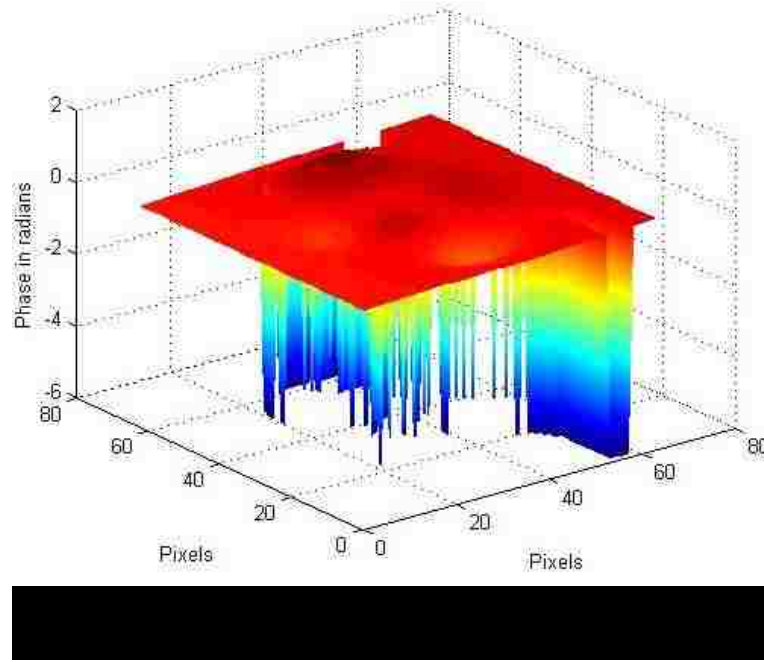
Calculating the phase of the ratio eq. (13) using the Andris equation (15) can be written as shown below:

$$\tan^{-1}\left(\frac{I_{2re}I_{1im} - I_{1re}I_{2im}}{I_{1re}I_{2re} + I_{1im}I_{2im}}\right) = \gamma\Delta B(TE_2 - TE_1) \qquad (42)$$

Equation (42) describes the resulting unwrapped phase which is the phase difference ($\Delta\varphi$) between the phase of images 1 and 2. The left hand side which is the Andris method uses the result of the ratio of both signals eq. (10) while the right hand side uses the direct form of subtraction between the correct phase of images 1 and 2 , where: the correct phase of images 1 is $-\gamma\Delta B TE_1$ and the correct phase of images 2 $-\gamma\Delta B TE_2$. Figure 5 below shows that both sides are equal: (a) the unwrapped phase using the Andris method and (b) the unwrapped phase using the direct subtraction between the correct phase of images 1 and 2.
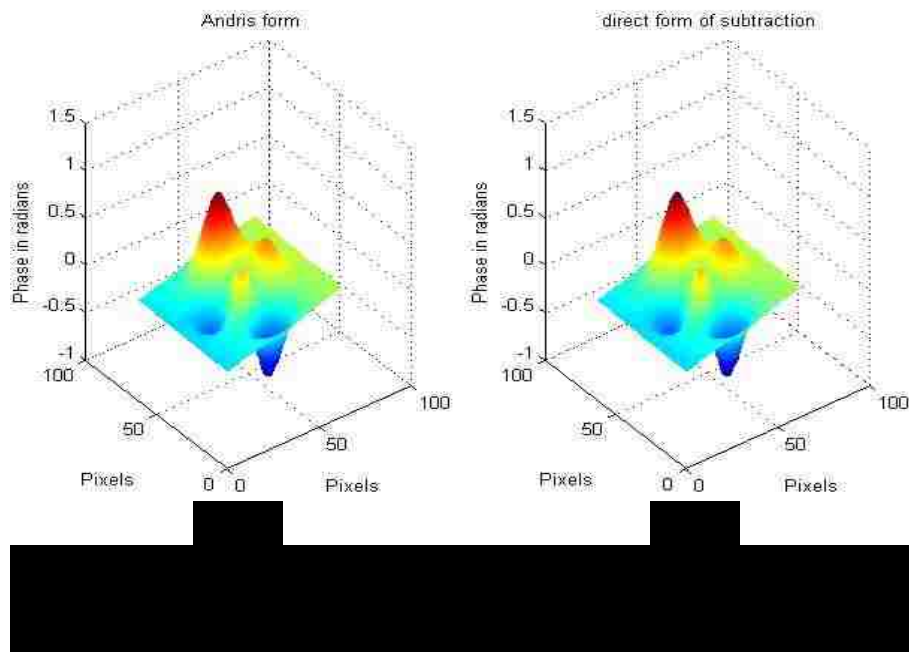
In the presence of noise (N), the accuracy of the Andris' method was evaluated and displayed in Figures 6 and 7.
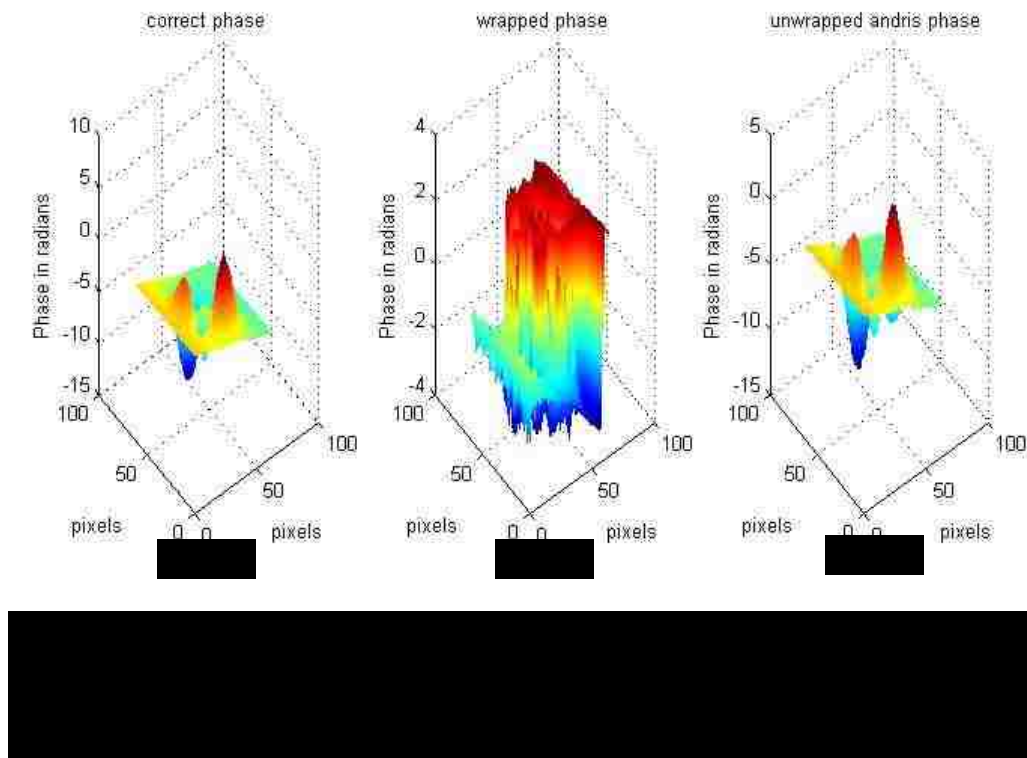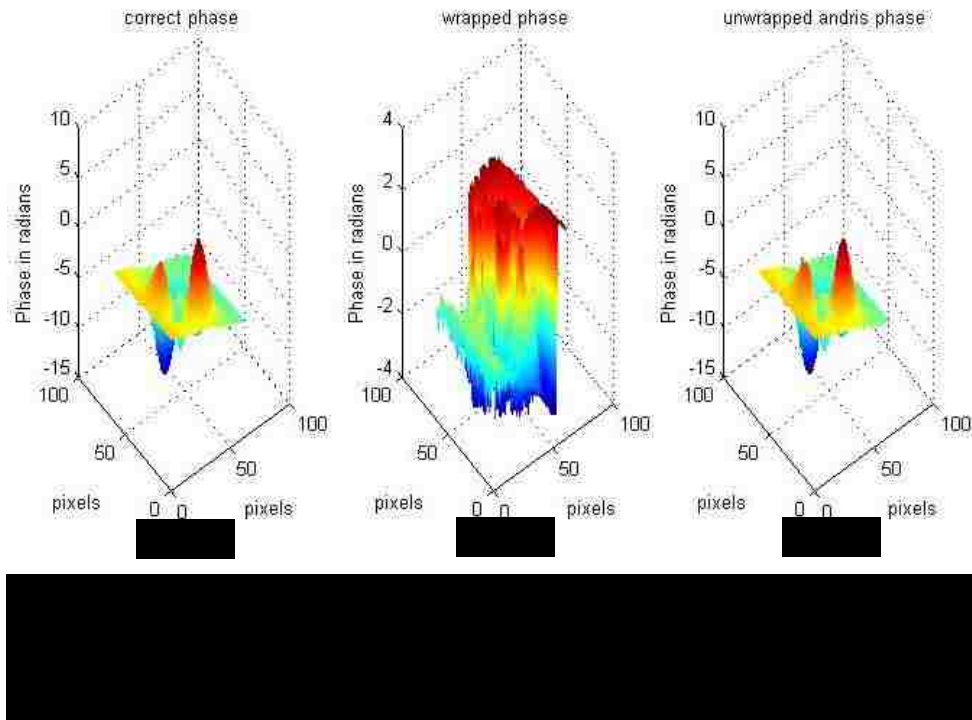
Figures 6 and 7 display the 3D phase images of the signals 1 and 2, at $\Delta B_0 = 10^{-7}T$, $\Delta TE_{12} = 2$ ms, $TE_1 = 20$ ms and $N = 0.3$. Figures 6(a) and 7(a) show the simulated correct phase of the signals 1 and 2, respectively. Figures 6(b) and 7(b) represent the wrapped phase of the signals 1 and 2, respectively, prior to applying the Andris' method. Figures 6(c) and 7(c) are the unwrapped phase of the two signals 1 and 2, respectively, after using the Andris method.

As mentioned previously in the chapter 2, there is a limitation in the performance of the Andris method when TEs are very long or the inhomogeneity ΔB is large, the resultant unwrapped image still has phase wrapping. The proposed algorithm is applied to a simulated MR image in the absence of noise and phase error and different inhomogeneity ΔB values. The results are shown in Figure 8.
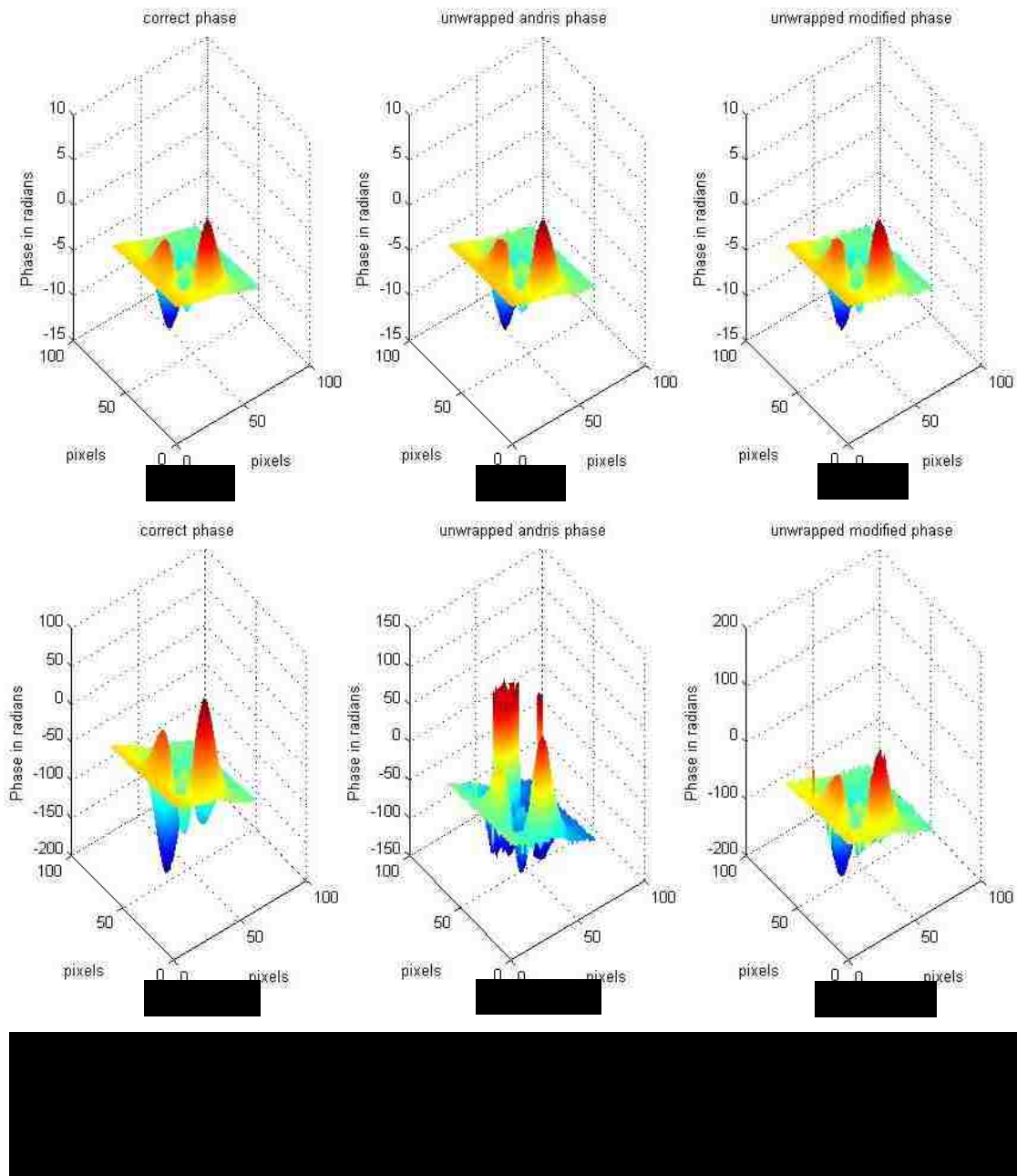
Figure 8 shows the 3D phase images of the signals 1 at $\Delta TE_{12} = 2$ ms, $\Delta TE_{23} = 1$ ms, and $N = 0.3$. (a) the simulated correct phase, (b) the unwrapped phase using the Andris method, and (c) the unwrapped phase using the modified method. The difference between two figures was the TE_1 and ΔB_0 values; (i) for small ΔB and short TE_1; $TE_1 = 20$ ms, $\Delta B_0 = 10^{-7}$ T, and (ii) for large ΔB and long TE_1; $TE_1 = 70$ ms, $\Delta B_0 = 5 \times 10^{-7}$ T. It should be noted that with increasing TE_1 and ΔB values the modified method was better than the Andris method.

3.1 Comparison between the Two Methods

A comparison in the performance of both methods is given below in terms of the error produced investigated as a function of many parameter such as TE, ΔTE, etc.

3.1.1 Echo Times (TE)

The investigation of the accuracy for both methods with different each time TE values is shown in Figure 9.
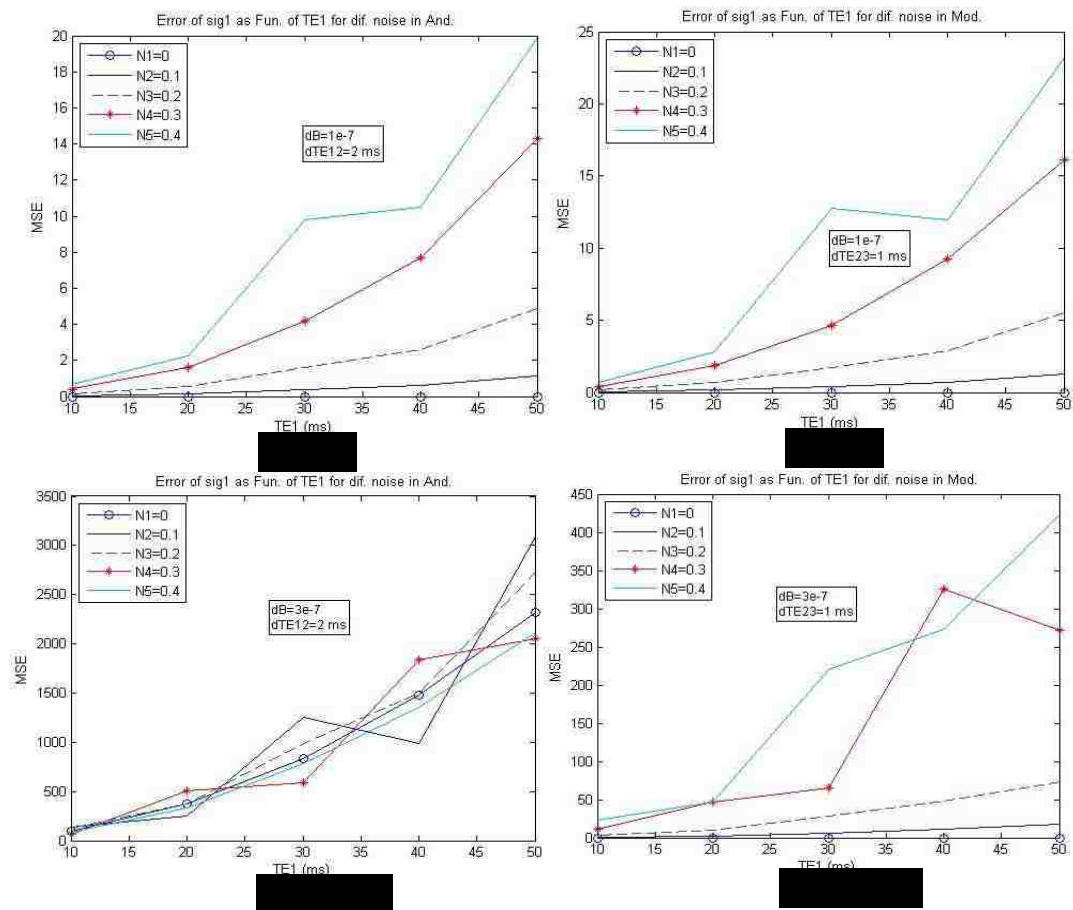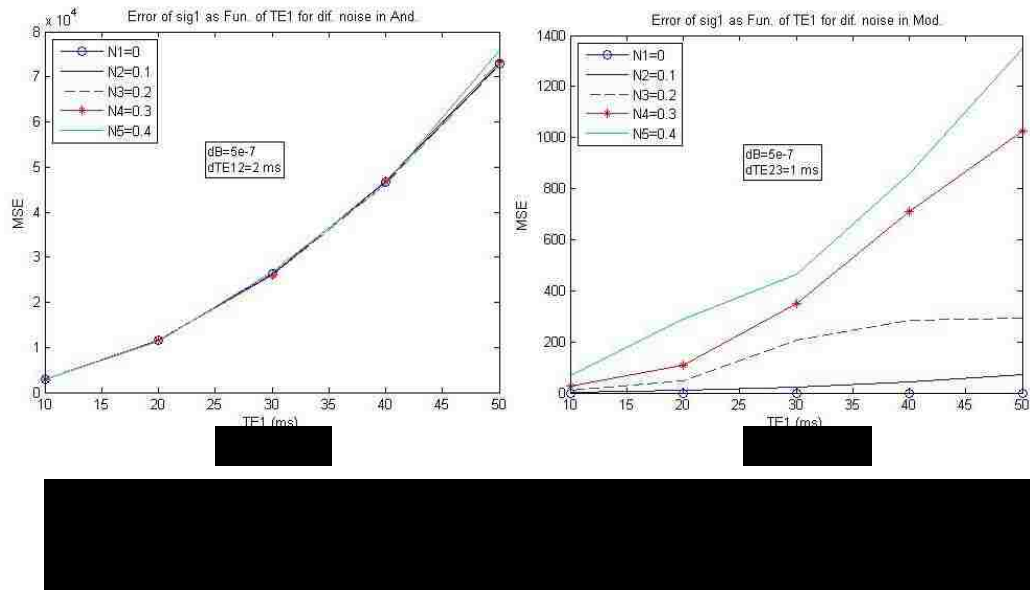
Figure 9 shows the MSE as function of TE_1 values of the signal 1 at $\Delta TE_{12} = 2$ms and $\Delta TE_{23} = 1$ ms for different noise values, using: (a) the Andris method; and (b) the modified method. The difference between the three sets of figures was inhomogeneity (ΔB) values; (i) $\Delta B_0 = 1 \times 10^{-7}T$, (ii) $\Delta B_0 = 3 \times 10^{-7}T$ and (iii) $\Delta B_0 = 5 \times 10^{-7}T$. It appears clearly that the MSE in both methods, in all figures, increases with rising TE_1 values but the MSE has more fluctuations in small ΔB, in Figures (i) and (ii), than in large ΔB, in Figure (iii). This is so because increasing TE_1 values causes more wrapping of the phase, and therefore it becomes more difficult for the routine to work. But it should be noted that the MSE in the modified method is smaller than in the Andris method. Also, it is obvious that the effect of the noise values in the Andris method disappears at large ΔB, i.e. the MSE is saturated and reached maximum value. Also noticeable is the large jump in the MSE values from $\Delta B_0 = 3 \times 10^{-7}T$ to $\Delta B_0 = 5 \times 10^{-7}T$ in the Andris method. The increase is more gradual in the modified method.

3.1.2 The Echo Time Differences (ΔTE)

The performance of the two methods with various echo time difference is shown in Figure 10.
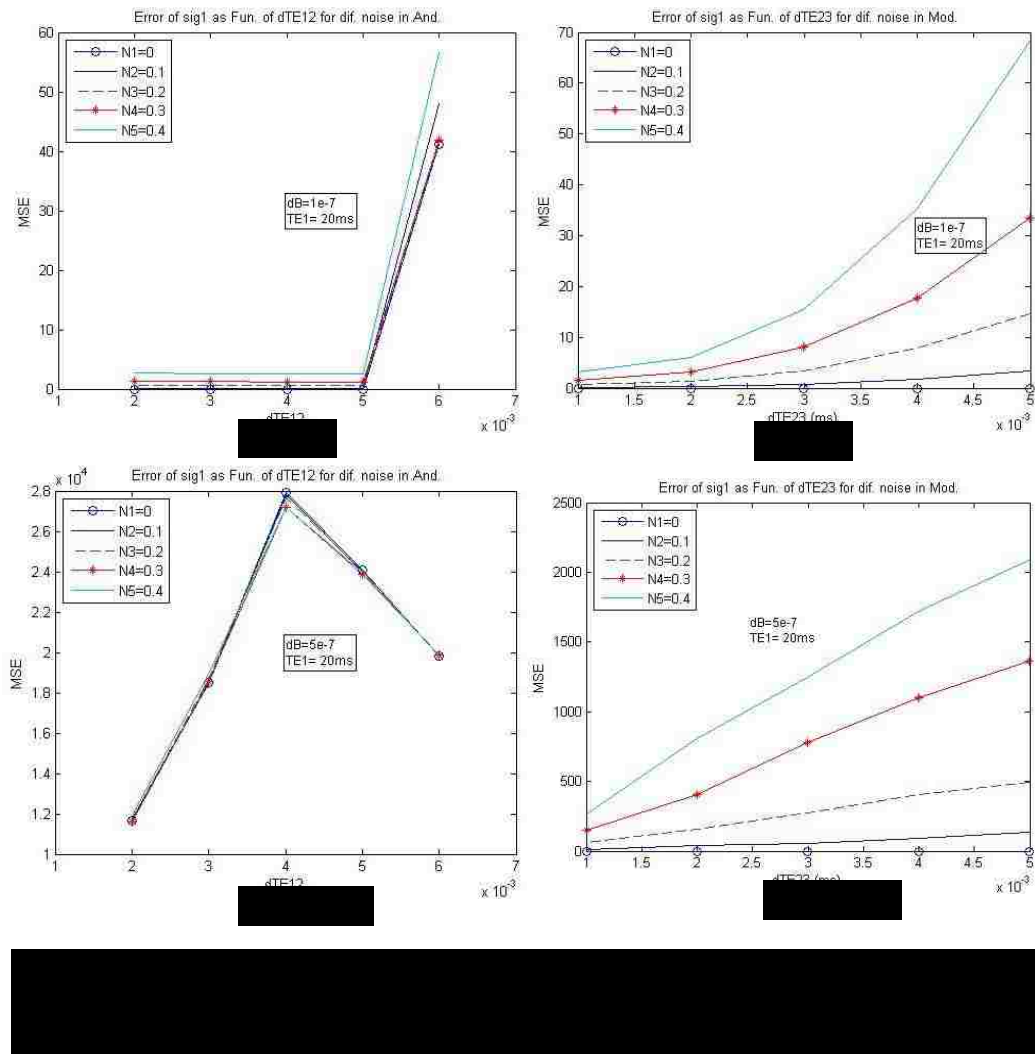
Figure 10 shows the MSE as a function of ΔTE for signal 1 at $TE_1 = 20$ ms and different noise values for different ΔB_0 value: (i) $\Delta B_0 = 10^{-7}$T and (ii) $\Delta B_0 = 5 \times 10^{-7}$T by using (a) the Andris method and (b) the modified method. In Figure 10(i) at smallΔB_0 there was a leveling out close to zero in the MSE as function of ΔTE_{12} in the Andris method until $\Delta TE_{12} = 5$ ms, then it starts increased rapidly.

While the MSE in the modified method rose steadily with increasing ΔTE_{23}. It should be noted that at small ΔB the Andris method performs better than the modified one. On the contrary, in figure 10(ii) at large ΔB, the MSE in the modified method is smaller than in the Andris' method. The MSE has a starting point above zero in the Andris method and it increased dramatically to reach a peak at $\Delta TE_{12} = 4$ ms, then fall steadily until $\Delta TE_{12} = 6$ ms. Conversely, the MSE in the modified method increases rapidly. It should be noted that there was small effect of increasing the noise values in Andris method unlike in the modified method, it has a large effect.

3.1.3 Noise (N)

The presence of noise will generate errors. The behavior of the two methods is represented in Figure 11.
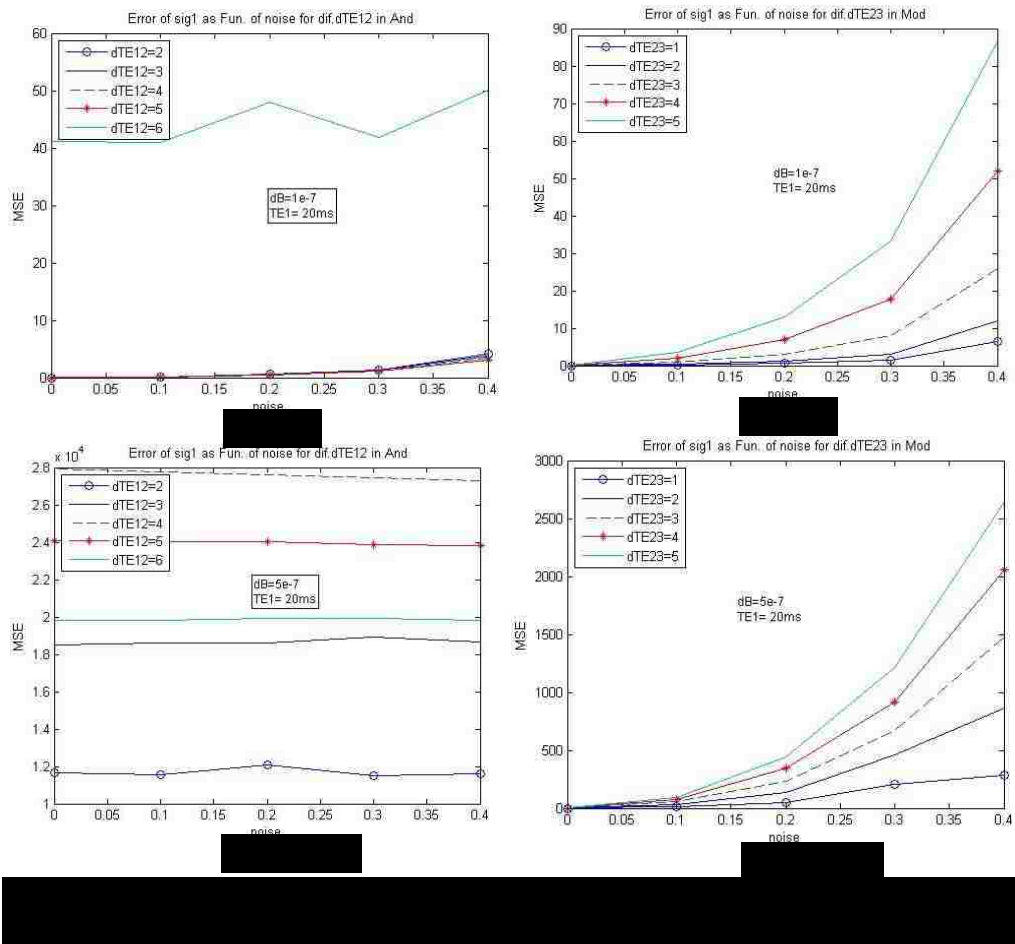
Figure 11 represents the MSE as function of noise for signal 1 at $TE_1 = 20$ ms for different ΔTE_{12}, ΔTE_{23} values, and different ΔB; (i) $\Delta B_0 = 10^{-7}T$ and (ii) $\Delta B_0 = 5 \times 10^{-7}T$ by using: (a) the Andris method and (b) the modified method. In the figure 11(i), it can be seen clearly that the MSE in the Andris method almost remained steady for different noise values while in the modified method there was a gradual rise in the MSE values with increasing noise values. The MSE in the Andris method is slightly smaller than the modified method. Also noticeable is the gap in the MSE in the Andris method between $\Delta TE_{12} = 5\ ms$ and $\Delta TE_{12} = 6\ ms$. In Figure 11(ii), it is obvious that at $\Delta B_0 = 5 \times 10^{-7}T$ the MSE in both method have the same behavior as, in Figure 11(i), at small ΔB except the variation with different ΔTE_{12} values is shown more clearly than previously. There was no big effect of increasing the noise values for the same ΔB in the Andris method while it appears clearly in the modified method. It should be taken into account that the modified method was much better than the Andris method because of the significantly smaller MSE.

3.1.4 Inhomogeneity (ΔB)

The effect of different inhomogeneity (ΔB) in the accuracy of both the Andris's and modified method were evaluated and displayed in Figure 12.
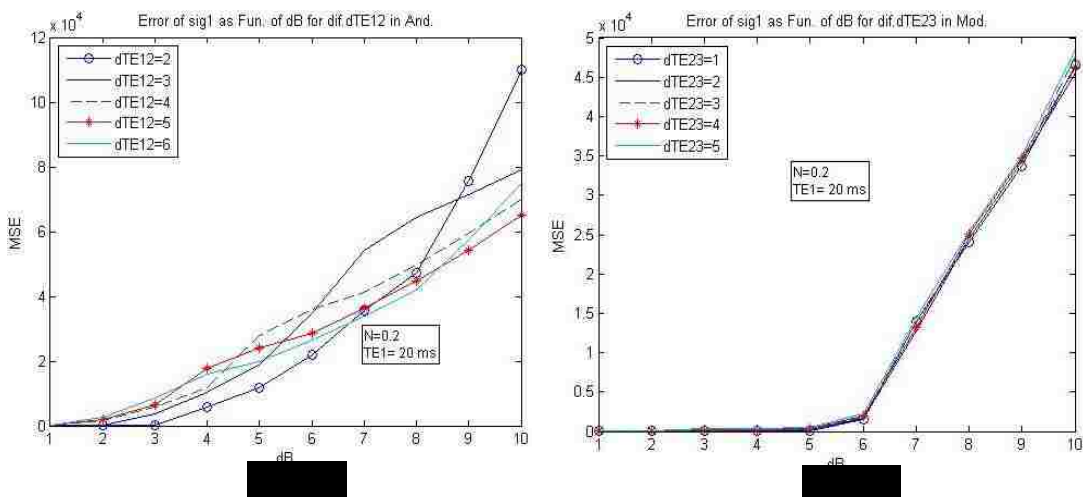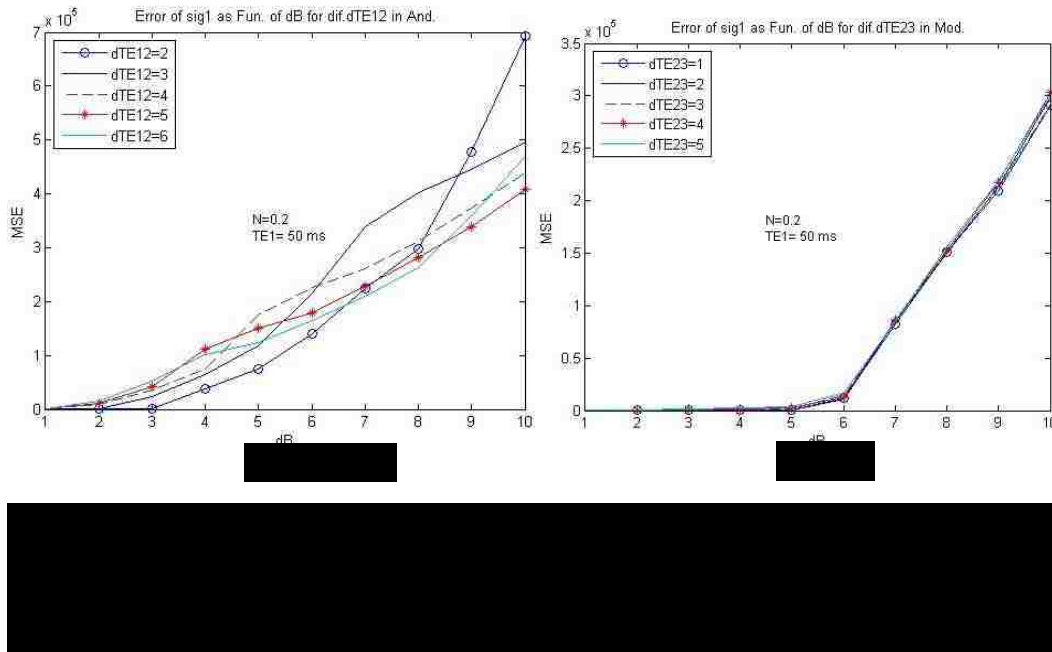
Figure 12 shows the MSE as function of ΔB for signal 1 at $N = 0.2$ at different TE_1: (i) $TE_1 = 20\ ms$ and (ii) $TE_1 = 50\ ms$ and for different ΔTE values: (a) at different ΔTE_{12} in the Andris' method and (b) at different ΔTE_{23} in the modified method. In general, it can be clearly seen that there was an upward trend with small fluctuations in the MSE, in the Andris method Figure 12 (i(a) and ii(a)), with increasing ΔB_0 values. The MSE values, in the modified method Figure 12 (i(b) and ii(b)), remained close to zero then increased sharply. Also, it should be noted that the MSE in the modified method is smaller than in the Andris method although different TE_1 used.

3.2 Phase Error $(\emptyset_{err})$

As we mentioned previously in the introduction, the phase error $(\emptyset_{err})$ appears due to gradients or RF sources and it may distort the results. To study the effect of presence the phase error $(\emptyset_{err})$, it was added to the phase of the images 1, 2, and 3, see equation (43) below.

$$I_i = \rho \exp(i(-\gamma \, \Delta B \, TE_i + \emptyset_{erri})) + Noise \qquad (43)$$

where $\emptyset_{erri}$ is the phase error as a linear function of x variable with amplitude A

$$\emptyset_{erri} = A_i \, x \qquad (44)$$

We will investigate if the Andris methods and the modified method can remove distortion or the error of gradients (or $\emptyset_{err}$). The result is shown in Figures (13-16).

wrapped phase · unwrapped andris phase · unwrapped modified phase
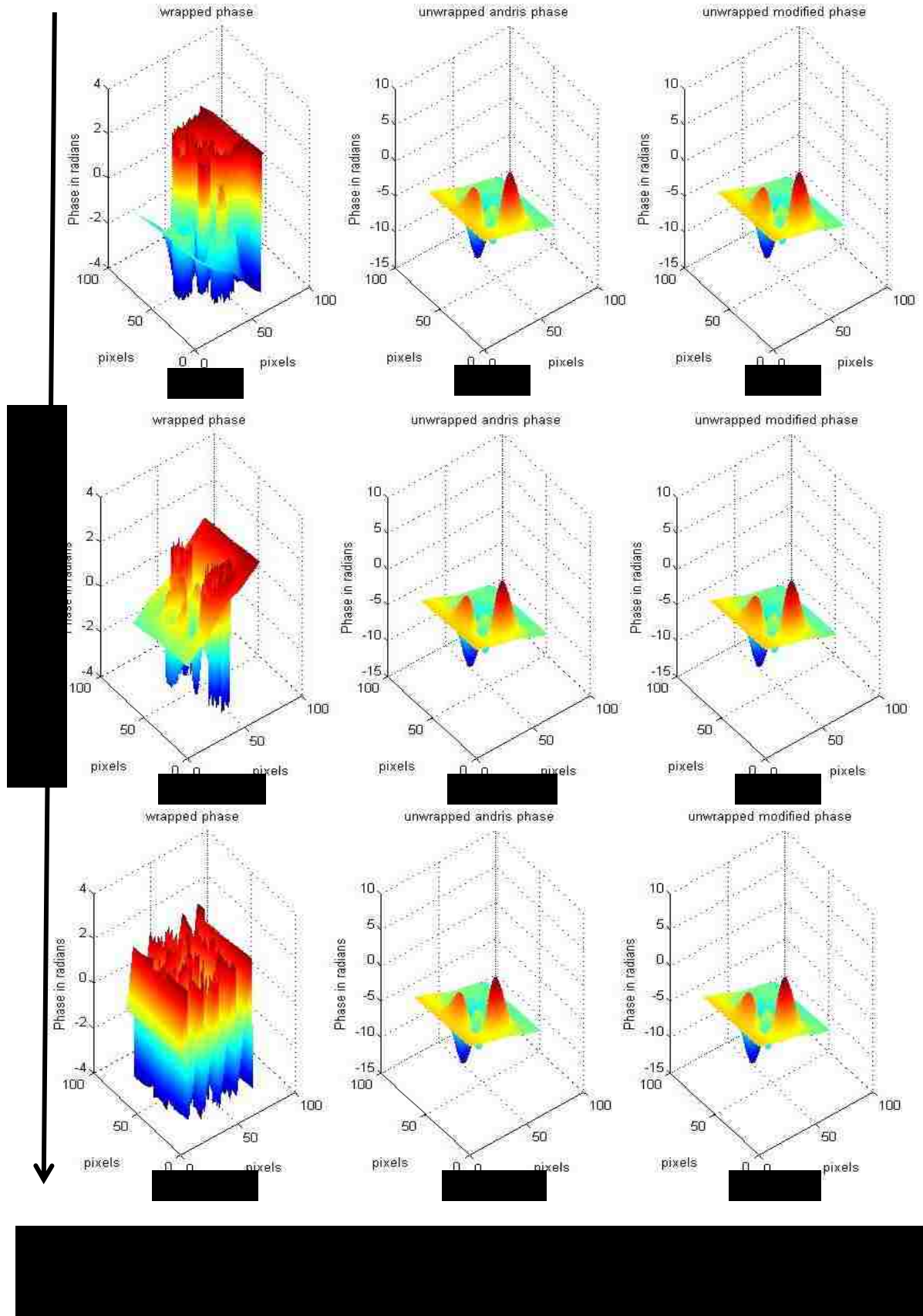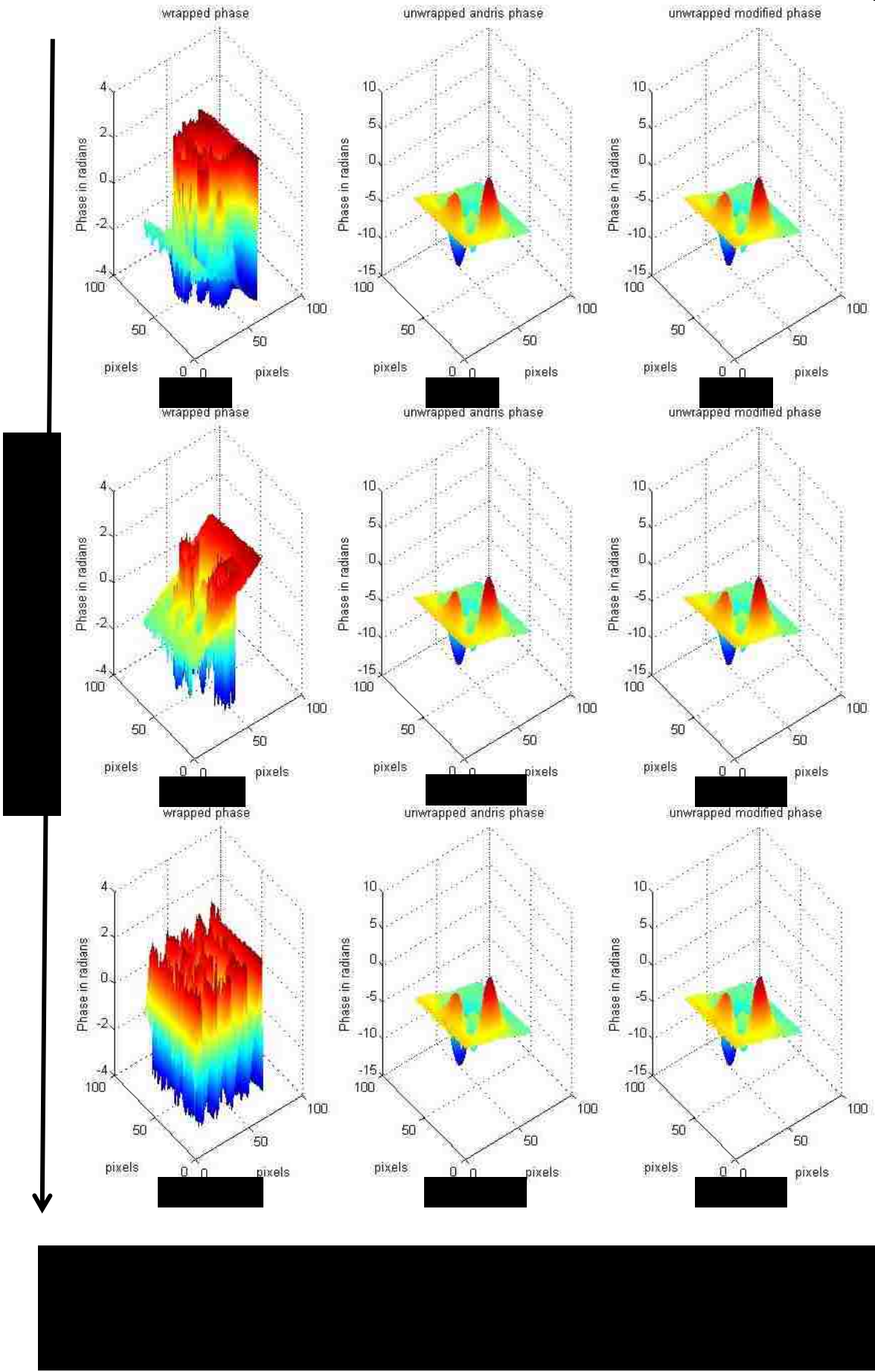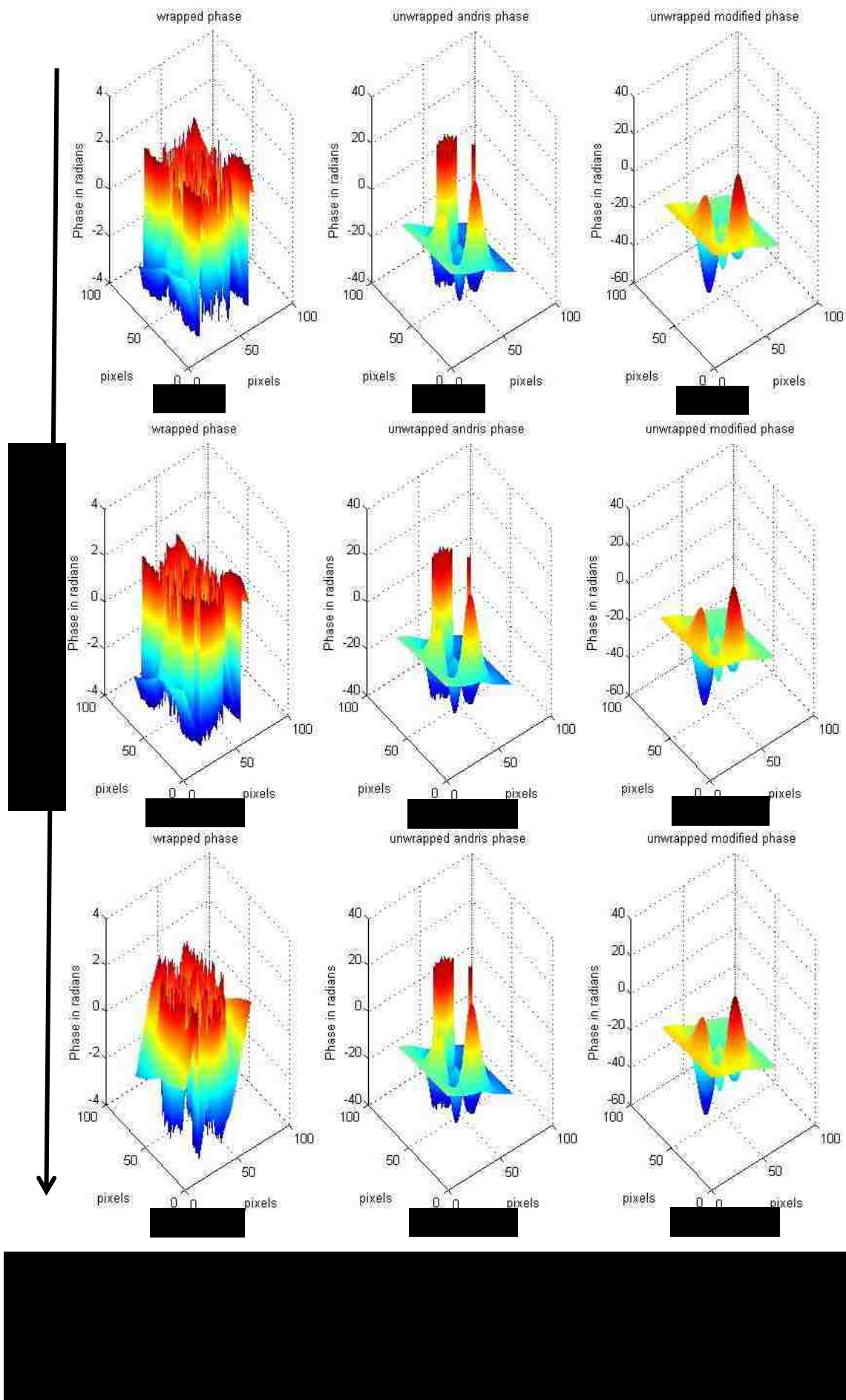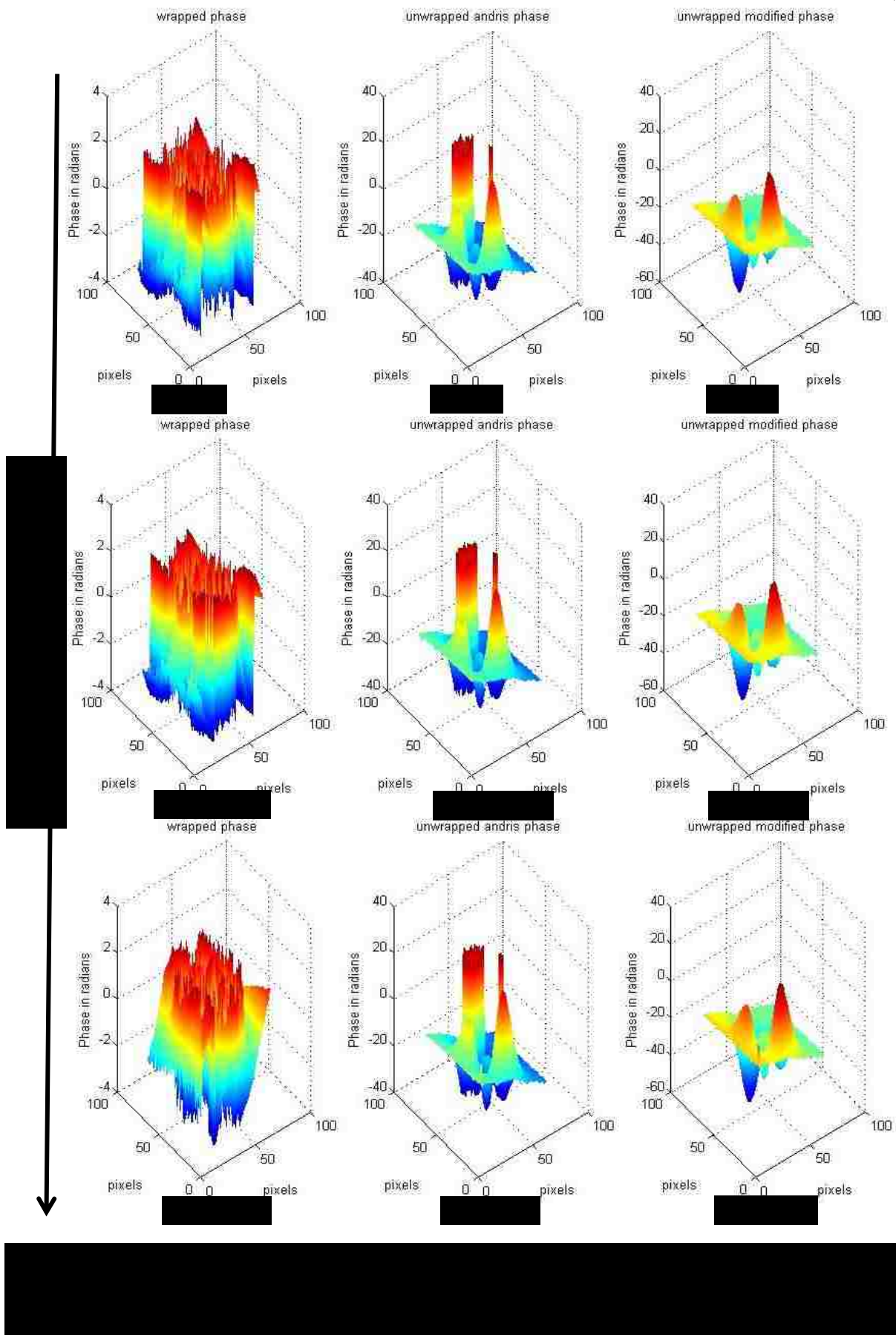
Figures (14-16) represent the 3D phase of the signal 1 at $TE_1 = 20$ ms and $\Delta TE_{12} = 2\ ms$, $\Delta TE_{23} = 1\ ms$, for different ΔB_0 values and phase error ($\emptyset_{err}$). In general, it can be seen clearly in all figures that both methods removed the effect of the gradients error whatever ΔB large or small and presence noise or not. In Figures (15-16) show that the modified method is better than the Andris it is not because the effect of the gradients error but it is due to the largeΔB.

The table (1) and (2) below show the MSE values of the signal 1 at $TE_1 = 20$ ms and $\Delta TE_{12} = 2\ ms$, $\Delta TE_{23} = 1\ ms$, for different ΔB_0 values and phase error ($\emptyset_{err}$). It can be seen clearly the effect of presence the phase error ($\emptyset_{err}$) was removed in both methods. The modified method is able to unwrap the phase with large inhomogeneity ΔB values.

Table 1: The MSE values and parameters at $\Delta B_0 = 10^{-7}$

ΔB_0 (T)	N	$\emptyset_{err}$	MSE	
			Andris	**Modified**
10^{-7}	0.0	0	0.0	0.0
		0.1 x	894.4	894.4
		0.5 x	2.24×10^4	2.24×10^4
	0.2	0	0.5552	0.6722
		0.1 x	894.71	894.40
		0.5 x	2.24×10^4	2.24×10^4

Table 2: The MSE values and parameters at $\Delta B_0 = 5 \times 10^{-7}$

ΔB_0 (T)	N	$\emptyset_{err}$	MSE	
			Andris	**Modified**
5×10^{-7}	0.0	0	1.17×10^4	0.0
		0.1 x	1.13×10^4	0.09×10^4
		0.5 x	2.77×10^4	2.24×10^4
	0.2	0	1.19×10^4	0.005×10^4
		0.1 x	1.12×10^4	0.09×10^4
		0.5 x	2.77×10^4	2.24×10^4

3.3 Evaluation of the Proposed Algorithm

In order to evaluate the efficiency of the proposed algorithm, three other different phase unwrapping algorithms were selected: Calibrated phase unwrapping based on least-squares and iterations (CPULSI), phase unwrapping method based on network programming (Costantini) and the Andris method. These algorithms and the modified were used to unwrap the phase image in two situations. The parameters were set to $TE_1 = 20$ and 50 ms, $\Delta B_0 = 10^{-7}$T and 5×10^{-7}T, and without phase error ($\emptyset_{err}$). The white noise (N = 0.02) was added into the phase directly, see eq. (45). The result is displayed in Figures 17 and 18.

$$I_i = \rho \exp(i(-\gamma \Delta B\ TE_i + Noise)) \tag{45}$$
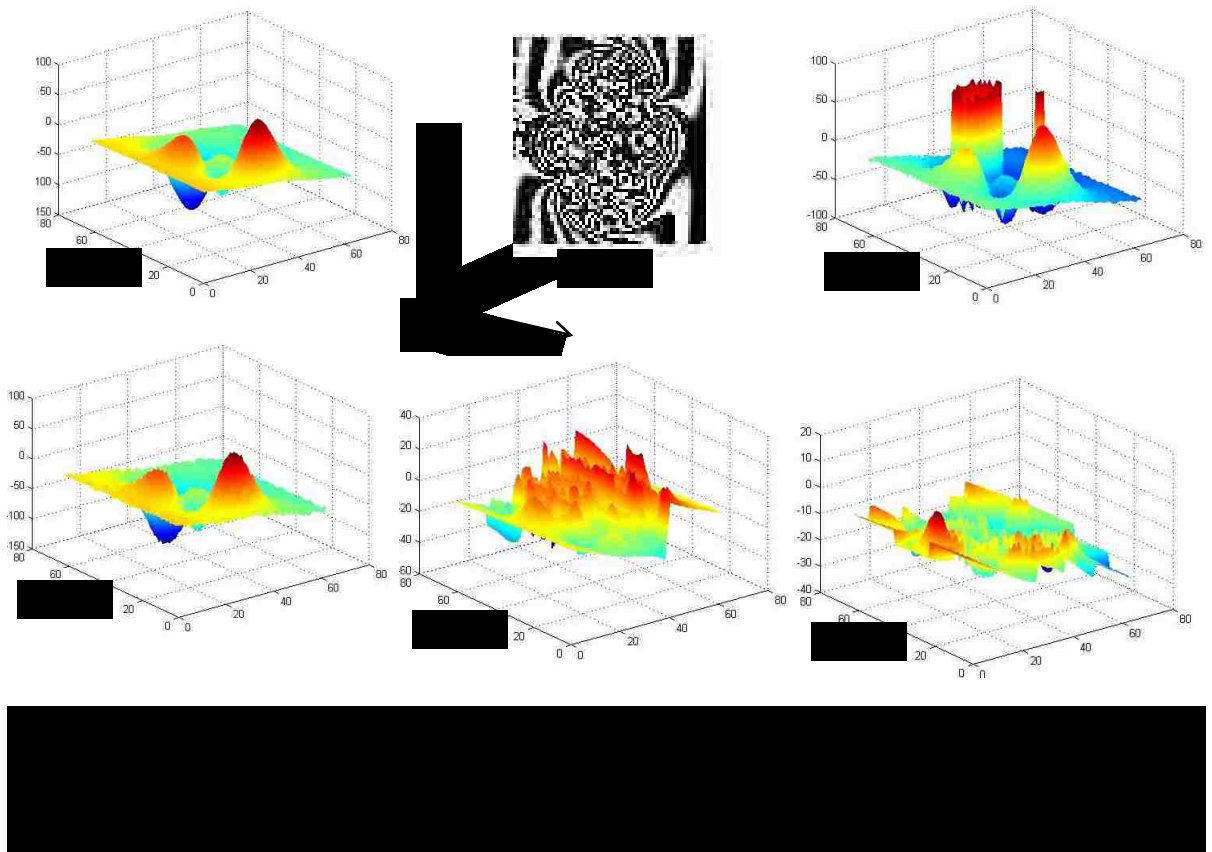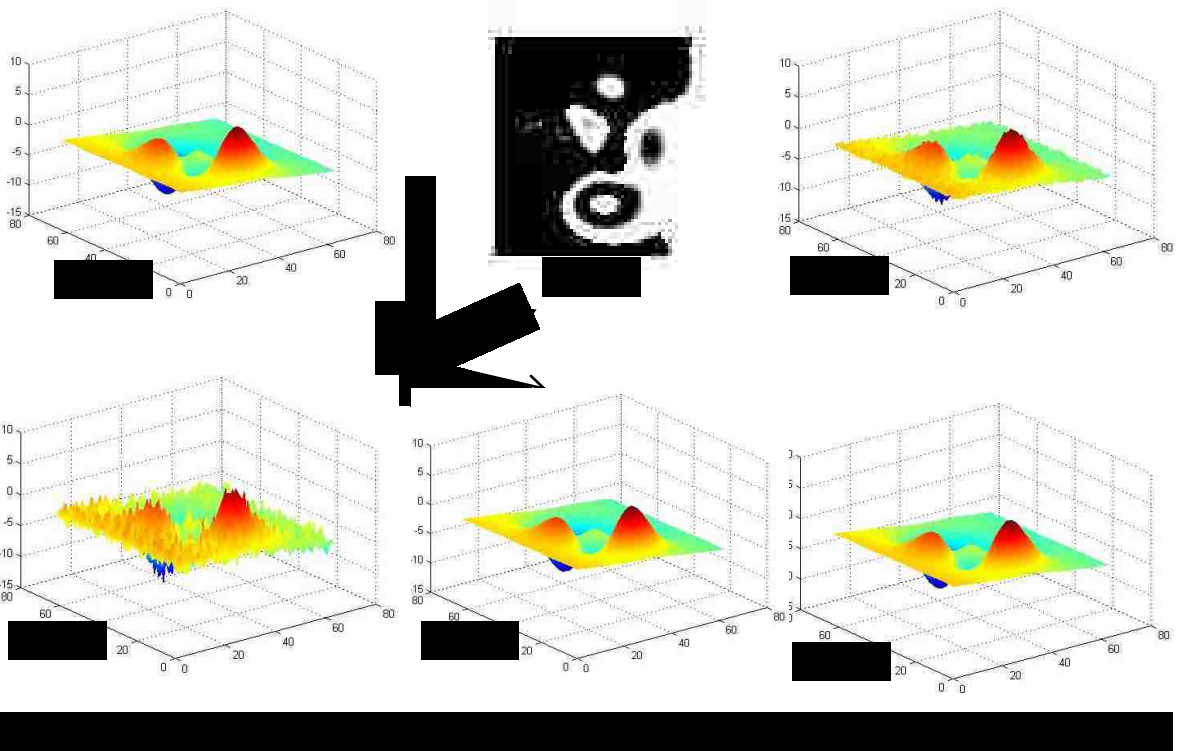
Figures 17 and 18 show the unwrapped phase using different algorithms with N = 0.02 for different ΔB and TE_1 value; (17) $\Delta B_0 = 10^{-7}T$ and $TE_1 = 20$ ms (18) $\Delta B_0 = 5 \times 10^{-7}T$ and $TE_1 = 50$ ms. (a) the simulated correct phase, (b) the wrapped phase (image), (c) the unwrapped phase using the Andris method, (d) the unwrapped phase using the modified method, (e) the unwrapped phase using method based on network programming (Costantini), (f) the unwrapped phase using Calibrated phase unwrapping based on least-squares and iterations (CPULSI). As can be seen in Figure 17, all algorithms exhibit very good unwrapped phase at small ΔB and short TE_1 while the effect of the noise appears clearly in the modified method in Figure 17(e). However in Figure (18) the only correct unwrapped phase with large ΔB and long TE_1 is obtained from the modified method. So, these simulated results given by the modified algorithm are better than those from the three other algorithms.

3.4 Justification of the Proposed Algorithm

In order to justify the implementation of the proposed algorithm, since it requires an additional image acquisition i.e. longer patient or experimental scan, we have to look at the practical execution of the scanner. Andris method relies on how small ΔTE_{12} can be (eq. (14)) and this is obviously a hardware constraints related to the ability of the gradient amplifiers (and other electronics) to raise and suppress the rapidly changing waveforms. Assuming the functional objectives of the scan require large TE values (e.g. $TE_1 = 40.0$ ms and $TE_2 = 42.0$ ms) then it is possible that the resulting wrapped phase is too large for the available minimum ΔTE_{12} (e.g. 2.0 ms). In order to remove the remaining wrapping we resorted to acquiring a third image at $TE_3 = 45.0$ ms. Notice that the condition of minimum ΔTE is not violated i.e. ΔTE_{23}

is not less than ΔTE_{12}. Inspecting the MSE reveals that the three image method yields a smaller error than the two image method 46953 versus 642 (at $\Delta B_0 = 5 \times 10^{-7}$T and noise level 0.2). Therefore, at the expense of acquiring an additional image the technique is now more powerful as shown by the results in unwrapping higher amplitudes of phase aliasing.

Chapter 4: Discussion

The purpose of this study is to investigate the performance of the modified phase unwrapping algorithm which is based on the Andris method. It was found that the modified algorithm is able to unwrap the phase with large ΔB or long TE_1, when other algorithms fail. Although the method is not the only approach, it has some advantages over others.

The Andris method allows distortions due to periodicity of the phase, generated by the mathematical method and due to hardware imperfection to be removed [9]. It removes the wrapping by shortening the effective echo time, however, this is limited by the flexibility of the pulse sequence. Also, the Andris method shows good accuracy in the presence of white noise especially when it was added into the signal. The limitation in the performance of the Andris method shows when the echo times (TE) is very long or the inhomogeneity (ΔB) is large. This makes the wrapping very severe. The modified method removes the wrapping phase by shortening the effective echo time as the Andris method but instead of using the difference of two echo times (TE), the modified method uses the differences between three echo times (TE). The Andris method is applied three times; in eq. (26), (28), and (30).

At small inhomogeneity (ΔB) and short echo times (TE), the performance of the Andris is better than the modified method with increasing the echo time difference (ΔTE) or the noise (N). As shown in figures 11(a) and 11(b), the effect of the noise (N) appears clearly in the modified method more than the Andris method. The MSE values increased with increasing the noise (N) values while in the Andris method remained steady. Increasing inhomogeneity (ΔB) or echo time (TE) causes

more wrapping of the phase and the inability of the Andris method to recover the uncorrupted phase. The noise is more effective in the modified method because it involves more mathematical processing. It is known that noise propagation increases with more mathematical steps.

Although the presence of noise (N) reduces the efficiency of the modified method, the MSE was smaller in the modified method than the Andris method at large inhomogeneity (ΔB) and long echo times (TE). As figure (12) demonstrates increasing the inhomogeneity (ΔB) effects clearly the performance of the Andris method while in the modified method the MSE remained closed to zero until large inhomogeneity ($\Delta B_0 = 6 \times 10^{-7}$T). Both methods removed the linear phase error ($\emptyset_{err}$) that appears due to gradients or RF sources regardless of ΔB large or small and the presence of noise or not.

In order to show the power of the proposed algorithm, comparison with two other established algorithms and the Andris method was carried out. This comparison shows that the modified method exhibits better accuracy with large ΔB or long TE_1, whereas others fail to unwrap. The method can be applied for MRI scanner or NMR tomography. Future studies should explore whether the modified method can achieve more efficient unwrapped phase by taking more than three signals with different echo times (TE).

Chapter 5: Conclusion

The modified method is an approach to successfully unwrap the phase and removes distortions of the periodicity of the phase, the gradient errors, and presence of the noise.

It is based on the Andris method but instead of using the difference between two echo times (TE) we use the differences between three echo times (TE). Although the modified method has the ability to eliminate the wrapping due to large inhomogeneity (ΔB) and long echo times (TE), the effect of the noise appears clearly in the method. The comparison to other algorithms shows that the modified method exhibit better performance with large ΔB or long TE_1, while others may fail. It can be used in the applications of MRI such as: field inhomogeneity mapping and flow imaging.

Future studies should explore whether the modified method can achieve more efficient unwrapped phase by taking more than three signals with different echo times (TE).

References

[1] A. V. Oppenheim and J. S. Lim, "The importance of phase in signals," *Proc. IEEE*, vol. 69, no. 5, pp. 529–541, May 1981.

[2] "Phase unwrapping," *Liverpool John Moores University*. [Online]. Available: http://www.ljmu.ac.uk/research/centres-and-institutes/faculty-of-engineering-and-technology-research-institute/geri/phase-unwrapping. [Accessed: 29-Mar-2017].

[3] M. Gdeisat and F. Lilley, "One-Dimensional Phase Unwrapping Problem," *ResearchGate*. [Online]. Available: https://www.researchgate.net/publication/265151826_One-Dimensional_Phase_Unwrapping_Problem. [Accessed: 29-Mar-2017].

[4] H. Xia, R. Guo, S. Montresor, J. Li, and P. Picart, "Unwrapping algorithm based on least-squares, iterations, and phase calibration to unwrap phase highly corrupted by decorrelation noise," in *Imaging and Applied Optics 2016 (2016), paper DW5E.8*, 2016, p. DW5E.8.

[5] H. Xia *et al.*, "Phase calibration unwrapping algorithm for phase data corrupted by strong decorrelation speckle noise," *Opt. Express*, vol. 24, no. 25, pp. 28713–28730, Dec. 2016.

[6] S. Robinson, H. Schödl, and S. Trattnig, "A method for unwrapping highly wrapped multi-echo phase images at very high field: UMPIRE," *Magn. Reson. Med.*, vol. 72, no. 1, pp. 80–92, Jul. 2014.

[7] M. Costantini, "A novel phase unwrapping method based on network programming," *IEEE Trans. Geosci. Remote Sens.*, vol. 36, no. 3, pp. 813–821, May 1998.

[8] P. Andris and I. Frollo, "MAGNETIC FIELD DISTRIBUTION MEASUREMENT IN NMR." Journal of ELECTRICAL ENGINEERING.

[9] P. Andris and I. Frollo, "Simple and accurate unwrapping phase of MR data," *Measurement*, vol. 42, no. 5, pp. 737–741, Jun. 2009.

Appendix

```matlab
%% developed Andris three images method
clear all
N = 64 ;        n=1:N;         [x,y]=meshgrid(1:N);
G = 42.6e6*2*pi;   %gyromagnetic ratio 2.675222005(63)×108 rad. s.
T^-1 or   42.6; %Mhz/Tesla
TE_1 = 20;          % echo time signal 1 in ms
TE_2 = 22;          % echo time signal 2 in ms
TE_3 = 23;          % echo time signal 3 in ms
TE1=TE_1.*1e-3; TE2=TE_2.*1e-3; TE3=TE_3.*1e-3;
delta_B =5e-7.*(2*peaks(N)+ 0.1*x + 0.01*y);
tmp=-G.*delta_B;   n_amp= 0.2;  er_grad=0.1*x;
% correct phases
  phas1=tmp.*TE1+er_grad;
  phas2=tmp.*TE2+er_grad;
  phas3=tmp.*TE3+er_grad;
  % correct phases + random error+gradiant error
 Noise = (n_amp)*(1+1i).*randn((size(phas1)));
image1 = ((2*peaks(N)+ 0.1*x + 0.01*y).* exp(1i.*phas1)+Noise);
image2 = ((2*peaks(N)+ 0.1*x + 0.01*y).* exp(1i.*phas2)+Noise);
image3 = ((2*peaks(N)+ 0.1*x + 0.01*y).* exp(1i.*phas3)+Noise);

% Real & Imaginary of Signals
R1 = real(image1);       I1 = imag(image1);
R2 = real(image2);       I2 = imag(image2);
R3 = real(image3);       I3 = imag(image3);
% Introduce wrapping by atan2
ph_wp1 = atan2(I1, R1);      % Wrapped phase of Signal 1
ph_wp2 = atan2(I2, R2);      % Wrapped phase of Signal 2
ph_wp3 = atan2(I3, R3);      % Wrapped phase of Signal 3


                             % M3: Eq(9) Andris Method
% the first different phase between TE1 and TE2
bot_factor1=I2.^2 + R2.^2;
RR12 =((R1.*R2) + (I1.*I2))./bot_factor1;
RI12 =((I1.*R2) - (R1.*I2))./bot_factor1;
R12 = RR12 + 1i*RI12;
ph_uwp12 = atan2(RI12,RR12);
% the second different phase between TE2 and TE3
bot_factor2=I3.^2 + R3.^2;
RR23 =((R2.*R3) + (I2.*I3))./bot_factor2;
RI23 =((I2.*R3) - (R2.*I3))./bot_factor2;
R23 = RR23 + 1i*RI23;
ph_uwp23 = atan2(RI23,RR23);
% the effective different phase between first and second differents:
bot_factor=RI23.^2 + RR23.^2;
RR13 =((RR12.*RR23) + (RI12.*RI23))./bot_factor;
RI13 =((RI12.*RR23) - (RR12.*RI23))./bot_factor;
R13 = RR13 + 1i*RI13;
ph_uwp_M = atan2(RI13,RR13);

%the phase of images after unwrapping:
delt_TE12 = TE2-TE1;   % effected delta_TE in original Andris method
delt_TE23 = TE3-TE2;
```

```matlab
delt_TE_eff = delt_TE23-delt_TE12;    % effected delta_TE in Modified Andris method

%%Andris's phases
ph_uwp1 = ph_uwp12*(TE1/(-delt_TE12));      % phase of image1 after unwrapping
ph_uwp2 = ph_uwp12*(TE2/(-delt_TE12));      % phase of image2 after unwrapping
ph_uwp3 = ph_uwp23*(TE3/(-delt_TE23));      % phase of image3 after unwrapping
%modified phases
ph_uwp1M =  ph_uwp_M*(TE1/(delt_TE_eff));      % phase of image1 after unwrapping
ph_uwp2M =  ph_uwp_M*(TE2/(delt_TE_eff));      % phase of image2 after unwrapping
ph_uwp3M =  ph_uwp_M*(TE3/(delt_TE_eff));      % phase of image3 after unwrapping

%% unwphM = G*delta_B*(-delt_TE_eff)
uwp_ph_M = G*delta_B*(-delt_TE_eff);

% Mean_square_error of modified
E1M =(phas1 - ph_uwp1M);              % Errors phase image1
E1_sq = (E1M).^2;                     % Squared Error image1
MSE1_M = sum(E1_sq(:))/N;             % Mean Squared Error of image1
% Mean_square_error of original
E1 =(phas1 - ph_uwp1);                % Errors phase image1
E1_sq = (E1).^2;                      % Squared Error image1
MSE1 = sum(E1_sq(:))/N;               % Mean Squared Error of image1
MSE =[MSE1 MSE1_M];disp(MSE)
figure(1),
subplot(1,3,1)
surf(x,y,ph_wp1, 'FaceColor' , 'interp' , 'EdgeColor' , 'none' ,'FaceLighting' , 'phong' )
xlabel('pixels' ), ylabel('pixels' ), zlabel('Phase in radians')
title('wrapped phase')
subplot(1,3,2)
surf(x,y,ph_uwp1, 'FaceColor' , 'interp' , 'EdgeColor' , 'none' ,'FaceLighting' , 'phong' )
xlabel('pixels' ), ylabel('pixels' ), zlabel('Phase in radians')
title('unwrapped andris phase ')
subplot(1,3,3)
surf(x,y,ph_uwp1M, 'FaceColor' , 'interp' , 'EdgeColor' , 'none' ,'FaceLighting' , 'phong' )
xlabel('pixels' ), ylabel('pixels' ), zlabel('Phase in radians')
title('unwrapped modified phase')
```